

# Delivery of Functional Anti-miR-9 by Mesenchymal Stem Cell-derived Exosomes to Glioblastoma Multiforme Cells Conferred Chemosensitivity

Jessian L Munoz<sup>1,2</sup>, Sarah A Bliss<sup>1,2</sup>, Steven J Greco<sup>2</sup>, Shakti H Ramkissoon<sup>3,4</sup>, Keith L Ligon<sup>3,4</sup> and Pranela Rameshwar<sup>2</sup>

Glioblastoma multiforme (GBM), the most common and lethal tumor of the adult brain, generally shows chemo- and radioresistance. MicroRNAs (miRs) regulate physiological processes, such as resistance of GBM cells to temozolomide (TMZ). Although miRs are attractive targets for cancer therapeutics, the effectiveness of this approach requires targeted delivery. Mesenchymal stem cells (MSCs) can migrate to the sites of cancers, including GBM. We report on an increase in miR-9 in TMZ-resistant GBM cells. miR-9 was involved in the expression of the drug efflux transporter, P-glycoprotein. To block miR-9, methods were developed with Cy5-tagged anti-miR-9. Dye-transfer studies indicated intracellular communication between GBM cells and MSCs. This occurred by gap junctional intercellular communication and the release of microvesicles. In both cases, anti-miR-9 was transferred from MSCs to GBM cells. However, the major form of transfer occurred with the microvesicles. The delivery of anti-miR-9 to the resistant GBM cells reversed the expression of the multidrug transporter and sensitized the GBM cells to TMZ, as shown by increased cell death and caspase activity. The data showed a potential role for MSCs in the functional delivery of synthetic anti-miR-9 to reverse the chemoresistance of GBM cells.

*Molecular Therapy—Nucleic Acids* (2013) 2, e126; doi:10.1038/mtna.2013.60; published online 1 October 2013

**Subject Category:** therapeutic proof-of-concept siRNAs, shRNAs, and miRNAs

## Introduction

Glioblastoma multiforme (GBM) is the most common and lethal cancer of the adult central nervous system. GBM cells uniformly acquire resistance to alkylating agents and to other antineoplastic treatments.<sup>1</sup> This resistance is associated with the upregulation of adenosine triphosphate-binding cassette drug efflux pumps.<sup>2</sup> MicroRNAs (miRs) can regulate a number of processes in GBM cells, such as chemoresistance and functional drug efflux.<sup>3</sup>

The miRs are small oligonucleotides, 18–22 base pairs long, which regulate gene expression.<sup>4</sup> They bind to the 3'- and 5'-untranslated regions of the targeted mRNAs to suppress translation. The functioning of miRs does not require complete complementarity. Furthermore, miRs have major, but parallel, roles in cell differentiation and oncogenic transformation.<sup>5</sup> Through the targeting of specific genes, miRs can behave functionally as tumor suppressors or oncogenes.<sup>6</sup>

miRs are upregulated in glioma cells and are involved in developmental processes.<sup>7</sup> Among these are miR-9 molecules that have been shown to suppress mesenchymal differentiation of GBM cells.<sup>7</sup> This report investigated the role of miR-9 in the resistance of GBM cells to temozolomide (TMZ). P-glycoprotein (P-gp) is involved in the chemoresistance of GBMs.<sup>8</sup> Furthermore, miR-9, through an indirect method, affected the increase in P-gp (unpublished data). This study assesses the feasibility of using anti-miR as a treatment to reverse the expression of P-gp and to sensitize otherwise-resistant GBMs to TMZ.

miR-targeting therapeutics in GBM is an area of extensive research.<sup>9</sup> Yet, functional delivery of these targeted treatments without the use of viral vectors is yet to be successful. Cell-based delivery mechanisms have become an attractive method for delivering miR and anti-miR for therapies, particularly through stem cells, due to their tropism to the region of GBM cells.<sup>10</sup> Neural stem cells and mesenchymal stem cells (MSCs) are currently in trials as drug delivery modes for GBM.<sup>11</sup> Although neural stem cells have been shown to be effective in drug delivery, the challenges of harvesting, expansion, and their immunogenic ability have limited their application in humans.<sup>12</sup> By contrast, MSCs, which are efficient in the delivery of drugs in cancer treatment, have added advantages in terms of ease of expansion, harvesting, and the ability to be transplanted into allogeneic host as 'off-the-shelf' cells.<sup>13</sup>

MSCs can communicate with cancer cells through gap junctional intercellular communication (GJIC) and also through secreted exosomes.<sup>14,15</sup> In this report, we show reversed chemoresistance of GBM cells to TMZ. We showed that this occurred by targeting of anti-miR through MSCs. In addition, we showed a significant role of MSC-derived exosomes in the transfer of anti-miR-9 compared with the GJIC between MSCs and GBM cells.

## Results

The purpose of the study is to determine whether MSCs can be used for providing treatment to GBMs. In addition, the plan is to determine whether delivery can occur through direct contact using the GJIC or indirectly through vesicles.

<sup>1</sup>Rutgers University—Graduate School of Biomedical Science, Newark, New Jersey, USA; <sup>2</sup>New Jersey Medical School, Newark, New Jersey, USA; <sup>3</sup>Department of Pathology, Brigham and Women's Hospital, Boston Children's Hospital, Boston, Massachusetts, USA; <sup>4</sup>Harvard Medical School, Department of Medical Oncology, Dana-Farber Cancer Institute, Boston, Massachusetts, USA. Correspondence: Pranela Rameshwar, Rutgers Biomedical Health Sciences, New Jersey Medical School, 185 South Orange Avenue, MSB E-585, Newark, New Jersey 07103, USA. E-mail: rameshwa@njms.rutgers.edu  
Received 23 April 2013; accepted 15 August 2013; advance online publication 1 October 2013. doi:10.1038/mtna.2013.60

Anti-miR was used for testing the effectiveness of the delivery method.

### Characterization of MSCs

Although MSCs can be isolated from a number of tissues and locations, the phenotypes are mostly uniform.<sup>16</sup> We showed the phenotypes of CD44, CD45, and CD105 and their multilineage capacity. Flow cytometric analyses indicated consistent expression of CD44 and CD105 and undetectable CD45, indicating nonhematopoietic bone marrow–derived cells (Figure 1a). Bright-field images of cultured MSCs indicated symmetrically shaped, fibroblastoid cells consistent with the characteristics of MSCs (Figure 1b; left panel).<sup>17</sup> The two lineages studied indicated efficient adipogenic and osteogenic differentiation, confirming the multipotency of the experimental MSCs (Figure 1b).

### Intercellular communication between MSCs and GBM cells

MSCs can have intercellular communication with other cell types.<sup>18</sup> These cells can communicate with GBMs through direct contact by GJIC and/or by contact-independent method. The latter entails communication through soluble factors and/or the secretion of vesicles. The two methods (Figure 2a) are shown as transwell cultures for contact-independent communication and as cocultures for direct intercellular communication (GJIC).

MSCs were labeled with the fluorescent CellTracker Orange (CMTMR ([5-(and-6)-(((4-chloromethyl)benzoyl)amino) tetramethyl-rhodamine]); Figure 2b) in both the cultures. In the contact-dependent method (cocultures), the GBM cells (U87 and T98G) were unlabeled. The transfer of CMTMR was studied using flow cytometry. After 72 hours, >85% of the dye was transferred to the GBM cells (Figure 2c; left panels versus middle panels).

The contact-independent (transwell) cultures, which contained upper and lower chambers, were separated by 0.4- $\mu$ m membranes (Figure 2a; left panel). The labeled MSCs were placed in the upper chambers and the unlabeled GBM cells were placed in the lower chambers. The MSCs could not migrate through the membranes. Unlike the cocultures, only ~16% of the dye was transferred from the MSCs to the GBM cells (Figure 2c; left panels versus right panels).

Intracellular CMTMR cannot be passively secreted from the MSCs to enter the GBM. Furthermore, the MSCs were >99% viable, thereby eliminating the release of CMTMR from nonviable MSCs. Therefore, the 16% dye transfer could occur only through MSC-derived vesicles. Thus, we showed intercellular communication between MSCs and GBM cells by two different mechanisms.

### Transfer of anti-miR-9 from MSCs to GBM cells through the GJIC

The literature indicated that small oligonucleotides, such as miRs, can be shuttled from one cell type to another through connexin-dependent GJIC.<sup>19</sup> miR-9 has been shown to be involved in neural development.<sup>20</sup> Because GBM cells generally reactivate neural developmental pathways,<sup>21</sup> we asked whether miR-9 was increased in GBM cells. If so, we would be able to take advantage of the intercellular communication between MSCs and GBM cells to target the miR-9.

We proposed that the resistant GBM cells will express miR-9. We therefore treated U87 and T98G with 200  $\mu$ Mol/l TMZ or vehicle. After 72 hours, the viable/resistant GBM cells were studied to know the miR-9 levels using real-time polymerase chain reaction (PCR). The values in the untreated cells were normalized to 1 and then used as the basis to calculate fold change in the TMZ-resistant GBM cells. The results indicated a significant ( $P < 0.05$ ) increase in the miR-9 levels of TMZ-treated GBM cells (Figure 3a).

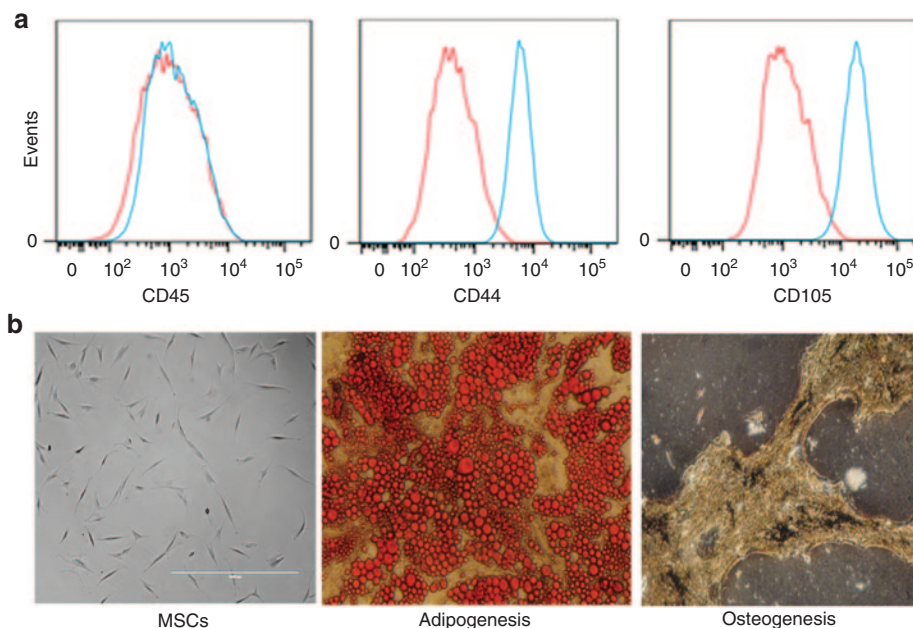


**Figure 1** Characterization of mesenchymal stem cells (MSCs). (a) Bone marrow–derived MSCs were analyzed by flow cytometry for CD45, CD44, and CD105 or (b) subjected to lineage differentiation. Left images show passage 5 MSCs at original magnification  $\times 100$ .

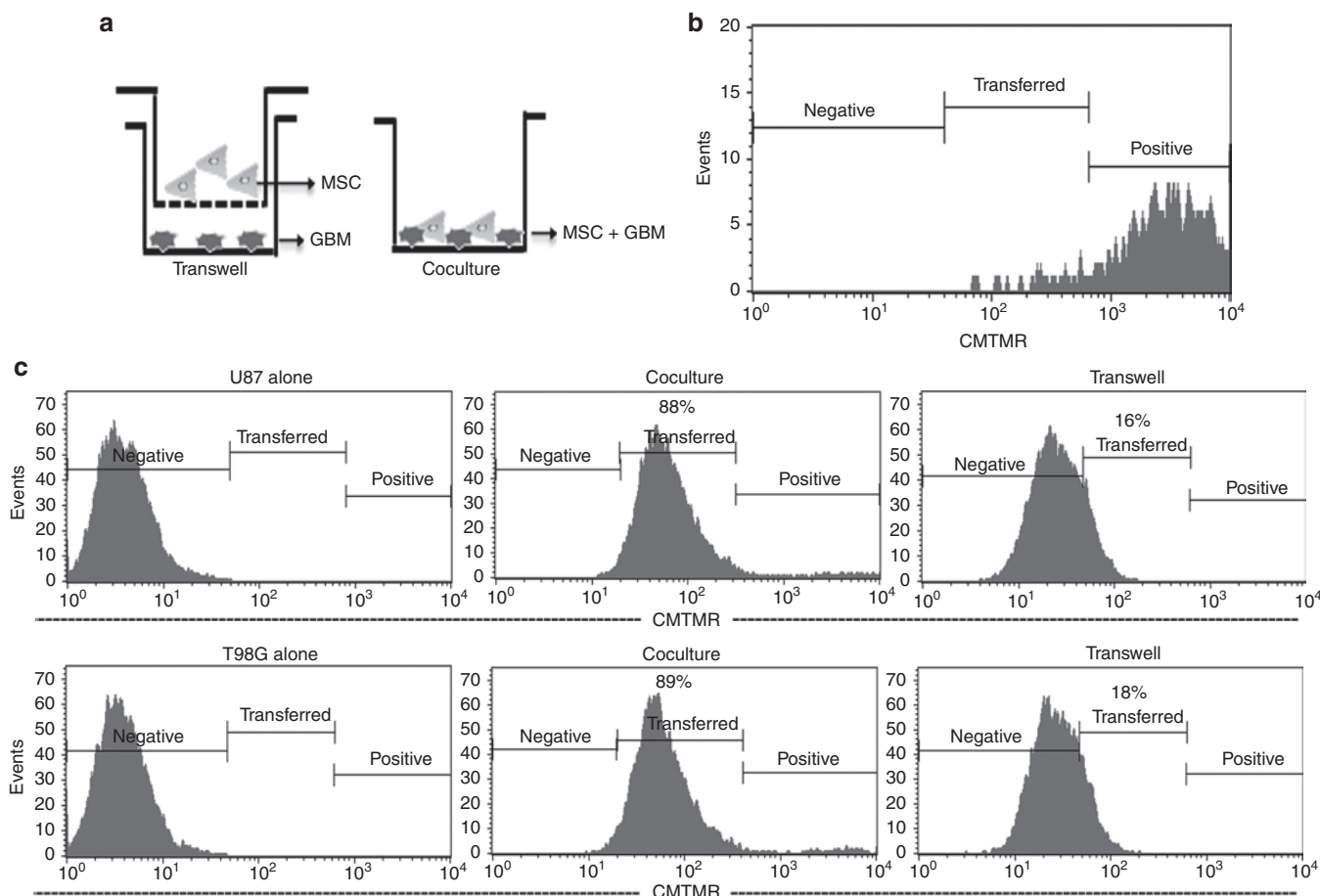


**Figure 2** Intercellular communication between mesenchymal stem cells (MSCs) and glioblastoma multiforme (GBM) cells. (a) The figure depicts the contact-independent transwell cultures and contact-dependent cocultures. (b) The cell tracker dye, CMTMR, was used to follow intercellular communication. The efficiency of loading CMTMR in MSCs is shown. (c) Flow cytometry for CMTMR in GBM cells in cocultures and transwell studies. CMTMR, [5-(and-6)-(((4-chloromethyl)benzoyl)amino) tetramethyl-rhodamine].

We next asked whether miR-9 can be blocked with anti-miR-9 and whether the anti-miR can be delivered through GJIC to the GBM cells. First, we investigated whether anti-miR can pass from MSCs to the GBM cells (T98G and U87) through the GJIC. To address this question, we synthesized anti-miR-9 tagged with Cy5. To identify the GBM cells, we labeled them with carboxyfluorescein diacetate (CFDA), which was not significantly transferred to the MSCs during the 72-hour incubation period (Figure 3b).

The transfer of Cy-5-anti-miR-9 was studied using flow cytometry. This was indicated by the detection of Cy5 in the CFDA-labeled GBM cells. As expected, no Cy5 was detected in the U87 and T98G cultured alone (Figure 3c,d; left panels). However, after coculture, the CFDA(+) GBM cells were also positive for Cy5 (Figure 3c,d; middle panels), indicating that anti-miR-9-Cy5 was transferred from the MSCs to the GBM cells. Histograms for Cy5 in the CFDA (+) GBM cells are shown in Figure 3c,d (right panels).

Because dye can be transferred from MSCs by a method other than GJIC (Figure 2), we asked whether the transfer of Cy-4-anti-miR-9 from the MSCs to the GBM cells occurred through GJIC. First, we asked whether connexin 43 (Cx43), which forms the GJIC, was present in cocultures of MSCs and

GBM cells. Immunocytochemistry resulted in bright labeling for Cx43 between the MSCs and the GBM cells (Figure 3e). We next performed cocultures in the presence of the GJIC blocker 300  $\mu\text{M}$ /l 1-octanol.<sup>22</sup> The control contained vehicle. The addition of 1-octanol resulted in 5–10% decrease in Cy5 fluorescence in the GBM cells (Figure 3f), indicating that there are also other mechanisms involved in the transfer of anti-miR-9-Cy5 to GBM cells. Due to the small decrease in the GJIC, we performed a control study with breast cancer cells, which can form GJIC at confluence.<sup>23</sup> Indeed, the presence of 1-octanol blocked the transfer of dye (Supplementary Figure S1). Taken together, these experiments indicated intracellular communication between the MSCs and the GBM cells and also suggested that other mechanisms of communication exist independent of the GJIC.

#### Contact-independent transfer of anti-miR-9-Cy5 from MSCs to GBM cells

Communication between cells may be contact dependent (GJIC) or contact independent (vesicular secretion). Figure 3 shows that many methods of communication other than GJIC may exist between MSCs and GBM cells. We therefore studied whether anti-miR-9-Cy5 was transferred from MSCs to

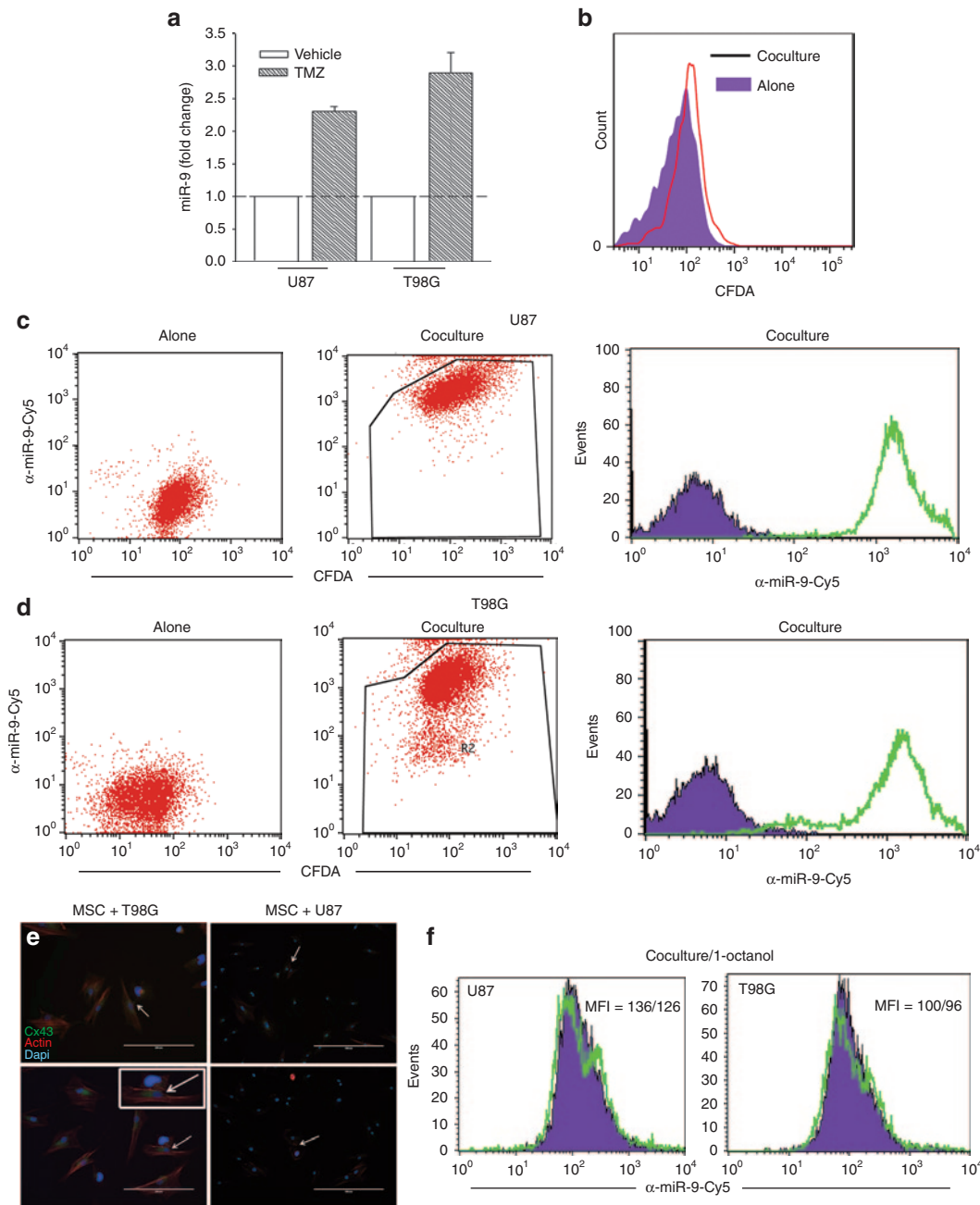


**Figure 3** Transfer of anti-miR-9-Cy5 from mesenchymal stem cells (MSCs) to glioblastoma multiforme (GBM) cells. (a) Real-time polymerase chain reaction for miR-9 in U87 and T98G, untreated and treated with 200  $\mu$ Mol/l temozolomide (TMZ). The data for the TMZ-treated cells are presented as fold change in relation to vehicle, which is normalized to 1. (b) GBM cells were labeled with the cell tracker CFDA and then placed in contact with MSCs. After 72 hours, the cells were analyzed for changes in Cy5. (c,d) Cocultures or transwell studies with anti-miR-9-Cy5-transfected MSCs and (c) CFDA-loaded U87 or (d) T98G were studied for the transfer of Cy5 probe. Left panels show the GBM cells alone; middle panels analyze the GBM cells for CFDA and Cy5; right panels show Cy5 alone in the GBM cells. (e) Representative immunocytochemistry is shown for Cx43 in cocultures of MSCs and U87 or T98G cells. The arrows show Cx43 (green) between two cells. Immediately before examining the cells, the cultures were labeled with phalloidin and diamidino-2-phenylindole. (f) Cocultures of U87 or T98G and MSCs were studied in the presence or absence of 300  $\mu$ Mol/l 1-octanol. After 72 hours, the cells were studied for Cy5.

the GBM cells in the transwell cultures (Figure 2a; left panel). We placed anti-mir-9-Cy5-transfected MSCs in the upper chamber and 5-chloromethyl fluorescein diacetate (CFDA)-labeled U87 and T98G cells in the lower chamber. After 72 hours, the GBM cells were collected and then analyzed by flow cytometry, as shown in Figure 3. The GBM cells cultured

alone were negative for Cy5 (Figure 4a,b; left panels). However, GBM cells in transwell cultures with the transfected MSCs showed Cy5 fluorescence in the CFDA(+) GBM cells (Figure 4a,b; middle panels). The histogram of Cy5 fluorescence from the transwell cultures is shown in Figure 4a,b (right panels). As the anti-miR-Cy5 can only enter the GBM

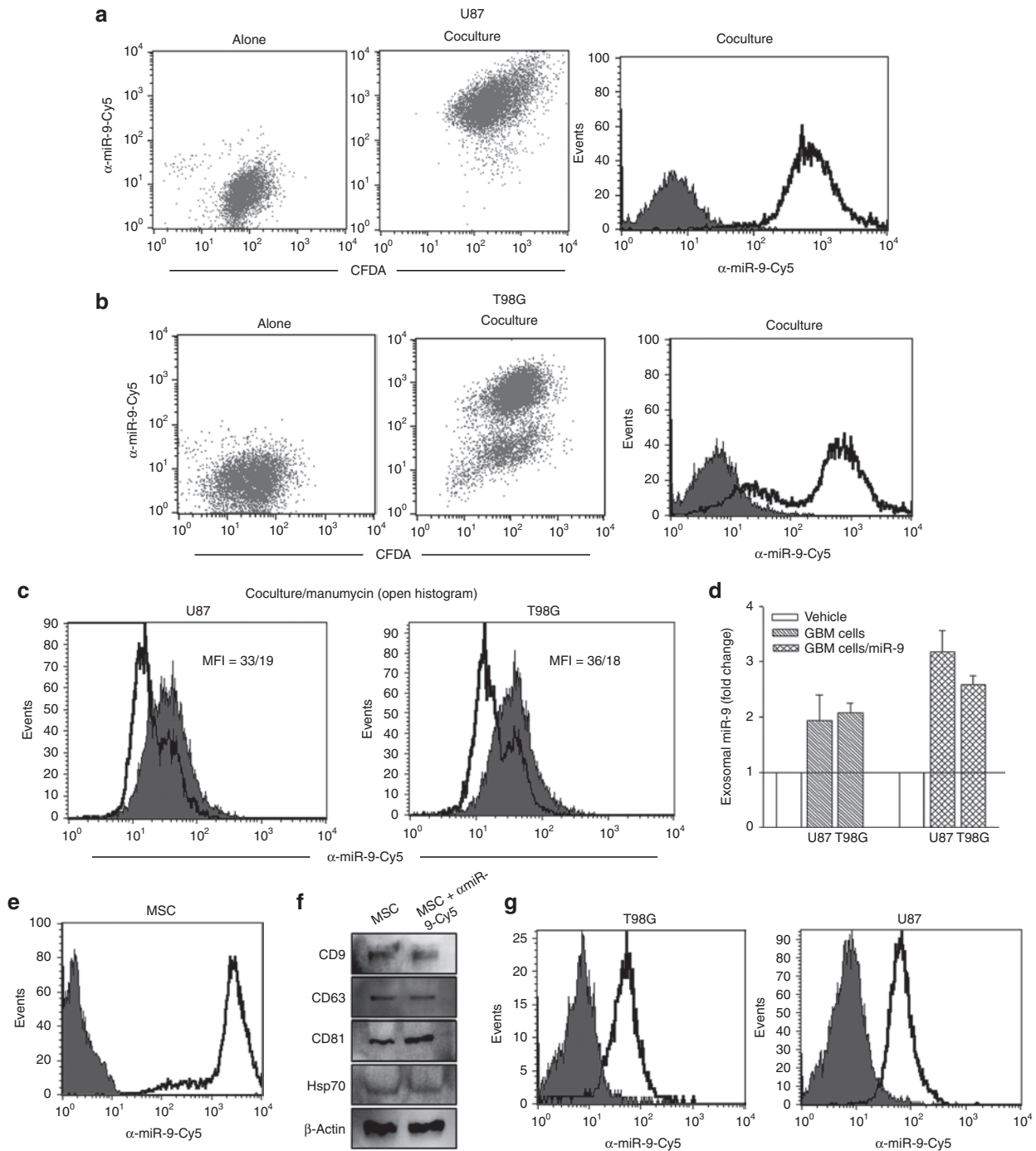


**Figure 4 Exosomal transport of anti-miR-9-Cy5 from mesenchymal stem cells (MSCs) to glioblastoma multiforme (GBM) cells.** (a,b) GBM cells were labeled with the cell tracker CFDA and then placed in the lower chambers of a transwell system. Anti-miR-9-Cy5-transfected MSCs were placed in the upper chamber of the transwell. After 72 hours, the cells were analyzed for changes in Cy5. Left panels show the GBM cells alone; middle panels analyze the GBM cells for CFDA and Cy5; right panels show Cy5 alone in the GBM cells. (c) Cocultures of U87 or T98G and MSCs were studied in the presence or absence of 300  $\mu\text{M}$ /l 1-octanol. After 72 hours, the cells were studied for Cy5. (d) Exosomal miR-9 from GBM cells was analyzed for miR-9 levels using real-time polymerase chain reaction. (e,f) MSCs were (e) transfected with anti-miR-Cy5 and then (f) characterized by western blot. (g) MSC-derived exosomes were added to GBM cells, and after 24 hours, the cells were examined for Cy5 by flow cytometry.

cells by vesicular transfer, the data suggest this type of transfer from MSCs to the GBM cells.

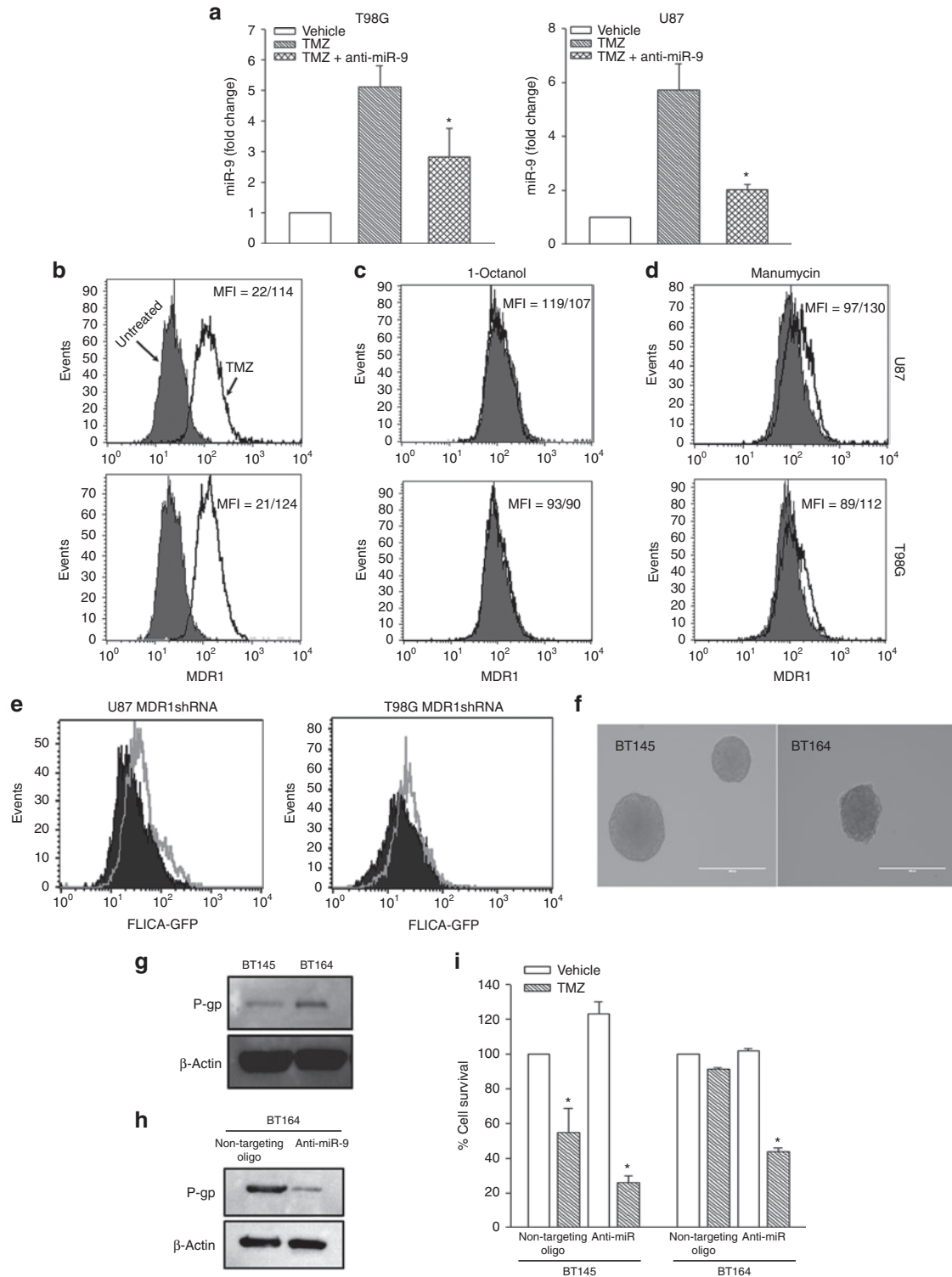
We performed studies to verify that anti-miR-9 was transferred by microvesicles. We repeated the transwell

cultures in **Figure 2**, except that we blocked the release of microvesicles using 2.5  $\mu\text{M}$ /l manumycin A (neutral sphingomyelinase 2, nSMase2).<sup>24</sup> Thus, the transwell cultures were established, as shown in **Figure 2a**, in the presence

or absence of manumycin A. The presence of manumycin A in the cultures reduced the fluorescence intensities (Figure 4c; open histograms) compared with the cultures without manumycin A (Figure 4c; solid histograms). The findings indicated that vesicular secretion was important for the transfer of anti-miR-Cy5 from MSCs to the GBM cells.

### Exosome-containing miR-9 from TMZ-resistant GBM cells

Figure 4a–c supports the role of vesicles in the transfer of anti-miR-9 from MSCs to GBM cells. We therefore extrapolated the findings to investigate how resistant GBM cells can sustain similar effects on neighboring GBM cells. To address



this, we collected exosomes from GBM cells, either untreated or treated with 200  $\mu\text{Mol/l}$  TMZ for 72 hours, and then studied the miR-9 levels using real-time PCR. TMZ treatment showed a twofold increase in exosomal miR-9 in the resistant U87 and T98G cells (Figure 4d). These findings indicated that chemoresistance could be influenced in the GBM cells through the release of miR-9-containing exosomes.

The increase in miR-9 in the exosomes of TMZ-treated cells could be caused by endogenous increase or by increase in the amount of secreted exosomes. To discriminate which method occurred, we collected exosomes from GBM cells, which were (i) either untransfected or with ectopic expression of miR-9 and (ii) untreated or treated with 200  $\mu\text{Mol/l}$  TMZ. The exosomes were studied for miR-9 levels using real-time PCR. The values in the untreated cells were normalized to 1, and the TMZ-treated cells were expressed as fold change. The results indicated significant ( $P < 0.05$ ) increase in miR-9 in relation to nontransfected, TMZ-treated GBM cells (Figure 4d). These findings indicated an increase in exosomal miR-9 by TMZ treatment. The findings in Figure 4d show that, in addition to an increase in miR-9 levels (Figure 3a), TMZ also increased vesicular secretion.

#### Direct transfer of exosomes from MSCs to GBM cells

The data in Figure 4a–d indicate that anti-miRs have the potential for therapy if they can be transferred by exosomes to GBM cells. We therefore investigated whether anti-miR-containing exosomes from MSCs can be transferred directly into GBM cells. We labeled MSCs with anti-miR-Cy5 (Figure 4e) and then collected exosomes from these MSCs. The exosomes were characterized using specific markers by western blotting (Figure 1f).<sup>25</sup> We added the MSC-derived exosomes to the GBM cells. As the exosomes were collected from anti-miR-Cy5-transfected MSCs, if the exosomes entered the GBM cells, this would be indicated by Cy5 fluorescence. Indeed, flow cytometry showed an increase in Cy5 (Figure 4g). A direct transfer of MSC-derived exosomes into GBM cells is thus possible.

#### Anti-miR-9 reversed MDR1 expression in TMZ-resistant GBM cells

Drug transporters are expected to be increased in TMZ-resistant GBM cells. We therefore asked whether an increase in miR-9 is important for the chemoresistance of GBM cells (Figure 3a). If so, inhibiting miR-9 with anti-miR is expected to decrease the expression of the drug transporter gene,

*MDR1*, resulting in reversal of TMZ resistance. First, we studied the functionality of the anti-miR-9-Cy5 by determining whether it can reduce the miR-9 level. We treated anti-miR-9-Cy5-transfected GBM cells with 200  $\mu\text{Mol/l}$  TMZ for 72 hours and then studied the levels of miR-9 using real-time PCR. Control cultures were treated with vehicle and were untransfected with anti-miR-Cy5. The untransfected/TMZ-treated cells showed approximately sixfold increase in miR-9 compared with the vehicle-treated ones (Figure 5a, diagonal bars). By contrast, anti-miR-9-Cy5 transfectants showed 50% decrease in miR-9 (Figure 5a, hatched bars), indicating that the anti-miR-9-Cy5 was able to functionally interact with miR-9 to decrease its level.

We next determined whether intercellular communication between MSCs and GBM cells (Figures 2 and 3) can be applied as a potential therapy. The goal was to determine whether the effect of miR-9 can be reversed with anti-miR-containing MSCs. If miR-9 is important for drug resistance, anti-miR-9 will reverse TMZ resistance and decrease *MDR1* expression. We performed cocultures with MSCs and GBM cells. The MSCs were transfected with anti-miR-9-Cy5, and the GBM cells were labeled with CFDA for the purpose of discriminating between the two cell types (Figure 3). The cocultures were treated with vehicle or 200  $\mu\text{Mol/l}$  TMZ in the presence or absence of 300  $\mu\text{Mol/l}$  1-octanol to block GJIC. After 72 hours, the cells were analyzed for surface P-gp (the *MDR1* gene product). TMZ-treated cells showed five- to sixfold more P-gp compared with untreated cells (Figure 5b). Parallel cocultures with 1-octanol resulted in minimum change in P-gp expression (Figure 5c). Because 1-octanol prevents the transfer of anti-miR-9-Cy5, the anti-miR was probably transferred by a method independent of GJIC. We therefore exposed the cocultures to 2.5  $\mu\text{Mol/l}$  manumycin A, which prevented vesicular release. Flow cytometry for P-gp showed a decrease in the mean fluorescence intensity (Figure 5d, shift from open histogram to solid histogram). The effect of manumycin A indicated that the transfer of anti-miR-9 occurred by vesicular transfer (Figure 4). Thus, anti-miR-9-Cy5 was functional and was transferred from MSCs to GBM cells, mostly through microvesicles. The transfer blocked the increase in P-gp.

#### Knockdown of P-gp in TMZ-resistant cells conferred apoptosis

Figure 5a,b shows the link between miR-9 and the expression of *MDR1*. To determine whether *MDR1* expression

**Figure 5 Anti-miR-9-Cy5 reversed glioblastoma multiforme (GBM) chemoresistance.** (a) Real-time polymerase chain reaction (Taqman) was performed with RNA extracted from GBM cells (T98G and U87). The cells were transfected with anti-miR-9-Cy5 and then treated with 200  $\mu\text{Mol/l}$  temozolomide (TMZ) or vehicle for 72 hours. (b) GBM cells were untreated or treated with TMZ as for “a.” The surviving resistant cells were labeled with CFDA dye, then cocultured with MSCs, and transfected with anti-miR-9-Cy5. After 72 hours, the cells were analyzed by flow cytometry for surface P-glycoprotein (p-gp; *MDR1*). (c) TMZ-resistant T98G and U87 were established as cocultures with MSCs as for “b,” in the presence or absence of 1-octanol. After 72 hours, the cells were analyzed for P-gp expression. (d) The cocultures in “c” were repeated, except in the presence or absence of manumycin. After 72 hours, the cells were analyzed by flow cytometry for P-gp. (e) U87 and T98G cells were stably knocked down for *MDR1* or a nontargeting vector (control). The transfectants were treated with 200  $\mu\text{Mol/l}$  TMZ. After 72 hours, the cells were analyzed for caspase 3/7 activity by flow cytometry using the Vybrant(R) FAM Caspase 3/7 Assay kit. Solid histogram: control; open histogram: *MDR1* knockdown. (f) Low-passage patient-derived cell lines (BT145, TMZ sensitive; BT164, TMZ resistant) are shown as nonadherent neurospheres. (g) Western blot was performed for P-gp using whole-cell extracts with the low-passage cell lines. (h) BT164 cells were transfected with anti-miR-9-cy5 and then analyzed for P-gp by western blot. (i) BT145 and BT164 cells were transfected with anti-miR-9-Cy5 or nontargeting anti-miR. The transfectants were treated with TMZ. After 72 hours, the cells were analyzed for viability using CellTiter–Blue assay. The viability with vehicle was normalized to 100% and then used as the base to calculate the percent change for the other experimental points; results are presented as mean  $\pm$  SD,  $n = 4$ . \* $P < 0.05$  versus vehicle.

is secondary to miR-9 for sensitivity to TMZ, we knocked down *MDR1* with short hairpin RNA (shRNA) and then studied whether this affected the sensitivity of GBM cells to TMZ. Controls were transfected with a nontargeting shRNA. The transfectants were treated with 200  $\mu\text{M}$ /l TMZ, and after 72 hours, the cells were analyzed for caspase-3/7. The results showed a shift in the positive direction, indicating increased apoptosis by the TMZ-treated cells (Figure 5e).

#### miR-9 in the sensitivity of low-passage GBM cells

The studies described above used established GBM cell lines. We asked whether the findings on miR-9 as a mediator of GBM resistance also occurred in low-passage

GBM cells. We addressed this question with two low-passage cell lines from patients: recurrent GBM that resisted TMZ (BT164 cells) and a cell line from a naive patient (BT145 cells). We first studied the expression of P-gp and observed an increase in the band in BT164 (Figure 5g). The P-gp band was significantly reduced when BT164 was transfected with anti-miR-9 (Figure 5h), indicating that miR-9 was responsible for the increase in P-gp. The decrease in P-gp with anti-miR also sensitized BT164 to TMZ (Figure 5i). The naive BT145 cells showed significant ( $P < 0.05$ ) cell death, regardless of transfection status (Figure 5i). In summary, the role of miR-9 in TMZ resistance was also noted for a low-passage recurrent GBM cell line from a patient.

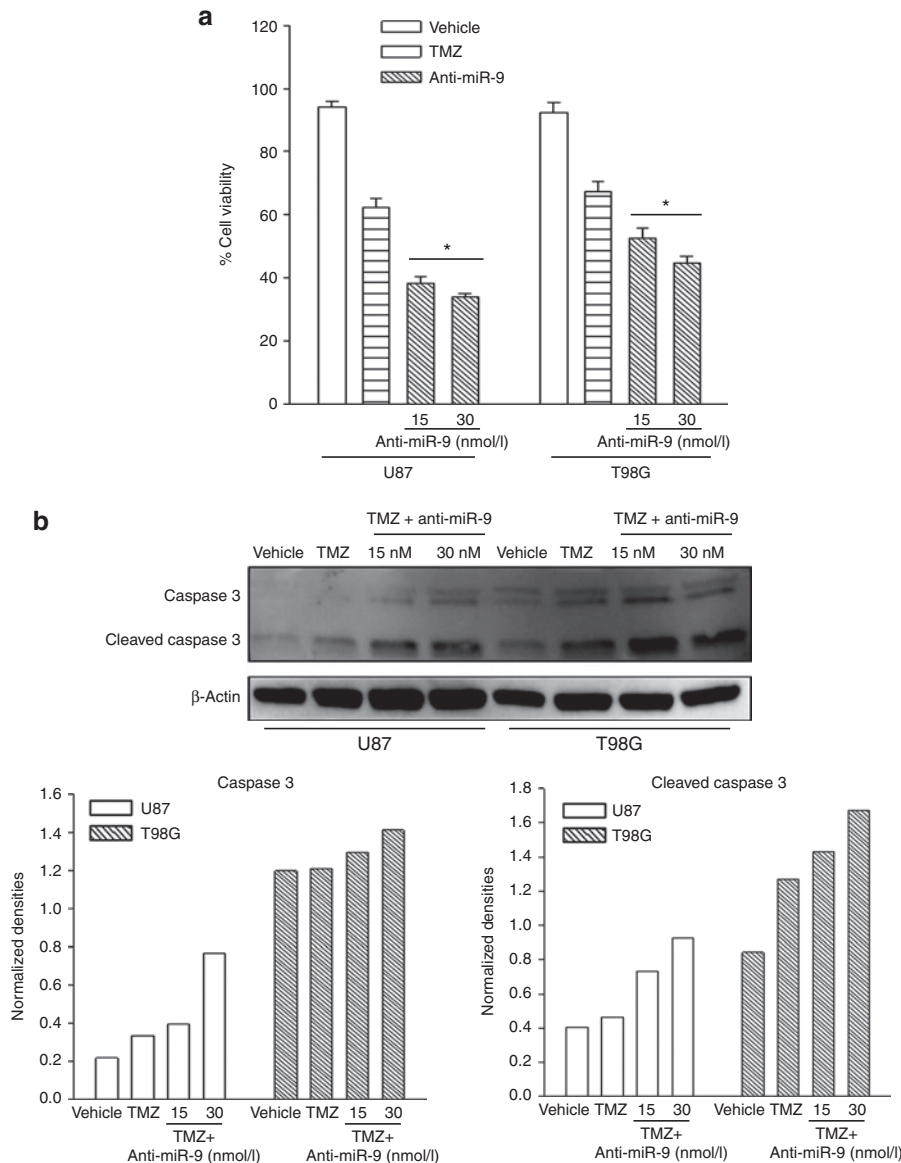


**Figure 6 Anti-miR-9 treatment enhanced temozolomide (TMZ)-induced cell death.** (a) Cell viability assay was performed with glioblastoma multiforme (GBM) cells treated with 200  $\mu\text{M}$ /l TMZ. The cells were transfected with anti-miR-9-Cy5 or nontargeted oligonucleotides. Adenosine triphosphate content was assayed by CellTiter-Blue assay. The data are presented as percentage cell viability  $\pm$  SD,  $n = 12$ . (b) Caspase-3 activity (caspase-3 cleavage) was studied by western blot (upper panel). The normalized band densities are shown in the lower graphs. \* $P < 0.05$  versus TMZ treatment alone.



### MSC-derived anti-miR-9 conferred sensitivity to TMZ on GBM cells

Because anti-miR-9 decreased the expression of *MDR1* (Figure 5), we asked whether anti-miR-9 can sensitize GBM cells to TMZ. U87 and T98G cells were transfected with 15 and 30 nM anti-miR-9-Cy5, respectively, and then treated with vehicle or 200  $\mu$ Mol/l TMZ. After 72 hours, cell viability was assessed with the CellTiter-Blue kit, and caspase activity was studied using western blotting. Cell viability was significantly ( $P < 0.05$ ) decreased with anti-miR-9-Cy5 treatment compared with TMZ treatment alone (Figure 6a).

Western blot analyses for uncleaved (35 kDa) and cleaved caspase-3 (17 kDa) showed an increase in the latter when the anti-miR-9-Cy5 transfectants were treated with TMZ (Figure 6b). The normalized band densities are shown in the lower graphs of Figure 6b. Altogether, the results indicated that anti-miR-9 increased active caspase and concomitantly caused enhanced cell death in response to TMZ treatment alone.

### Discussion

Refractoriness of GBM cells to chemotherapy and enhanced tumor growth commonly occur in GBM cells.<sup>26</sup> Several studies and clinical trials have used stem cells for delivering drugs to the sites of GBMs. These include current experimental therapeutics to deliver targeted prodrugs or genes. Human MSCs have been shown to exhibit tropism for the site of GBM. The chemoattraction of MSCs has been shown to depend on a number of chemokines and other cytokines, such as interleukin-1 and stromal derived factor-1 (SDF-1/CXCR4). In this article, we report on a potential RNA therapy for the neurodevelopmental miR-9 through the delivery of MSCs to make GBMs sensitive to TMZ.

We used human bone marrow-derived MSCs with anti-miR tagged with Cy5 to show effective transfer of the anti-miR from MSCs to GBM cells. This occurred through contact-dependent (GJIC) and contact-independent mechanisms (Figures 3 and 4). Because transfected MSCs remained viable, the Cy5 could not be derived from nonviable cells but could only be derived through regulated transfer. We showed a role for secreted exosomes in the communication between MSCs and GBM cells (Figures 4 and 5). The MSCs were multipotent and expressed Cx43 (Figures 1 and 3d). We used Cy5-tagged anti-miR-9 for tracking the transfer of the molecules. We demonstrated that the anti-miR-9 could decrease miR-9 and also reduce the resistance of GBMs to TMZ (Figure 6). This increased sensitivity of the anti-miR-9-containing GBMs correlated with the expression of the drug transporter P-gp (*MDR1*; Figure 5). The use of transwell cultures and flow cytometric analyses indicated that the ability of anti-miR-9 to make the cells chemosensitive could be applied by delivering the anti-miR through MSCs. The transfer was seen to be primarily through exosome-dependent intracellular communication rather than GJIC (Figure 5). This is a significant finding because the release of exosomes would be able to affect GBM cells that are at a considerable distance from the MSCs.

Anti-miR-9 delivered to the TMZ-resistant GBM cells was able to reduce the endogenous upregulation of miR-9 in

response to TMZ, in addition to significantly reducing cell surface P-gp. This protein is the product of the drug transporter *MDR1*, which is commonly associated with chemoresistance of cancer cells (Figure 5). Furthermore, we assessed the effects of anti-miR-9-Cy5 in the sensitization of GBM cells to TMZ. We transfected GBM cells with anti-miR-9-Cy5 and treated them with TMZ for 72 hours. Cell death was measured by adenosine triphosphate content (CellTiter-Blue assay) and caspase activity (western blot). The results indicated an enhancement of cell death when the anti-miR-9-Cy5 was combined with TMZ compared with the level of cell death with TMZ alone (Figure 6).

The field of RNA therapeutics has yet to identify a specific-target approach to GBM by anti-miR delivery. In this report, we showed the feasibility and the effectiveness of MSC-targeted delivery of anti-miR for GBM chemoresistance. The innate tropism of MSCs for GBMs and the ability of allogeneic MSCs to be used as off-the-shelf stem cells make the findings exciting because the method has potential for use in therapy.

### Materials and methods

**Reagents.** All tissue culture media were purchased from Gibco (Grand Island, NY); fetal calf serum was from Hyclone Laboratories (Logan, UT); TMZ, 1-octanol, and manumycin A were from Sigma Aldrich (St. Louis, MO), and lipofectamine RNAiMax was from Invitrogen (Grand Island, NY). Anti-microRNA-9-Cy5 (5'-Cy5-TCA TAC AGC TAG ATA ACC AAA G-3') was synthesized by Sigma Aldrich.

Murine anti-human P-gp (UIC2 clone)-PE was purchased from Biologend (San Diego, CA); anti-CD45-PE, anti-CD44-APC, and anti-CD45-V450 from BD Biosciences (San Jose, CA); and anti-caspase 3 from Cell Signaling (Danvers, MA).

**Cells.** U87 and T98G cells were purchased from American Type Culture Collection (Manassas, VA) and then grown as per manufacturer's instructions. As of 2007, histopathological analyses of both cell lines confirmed the diagnosis of Astrocytoma grade 4 (GBM).

BT145 (primary GBM) and BT164 (recurrent GBM) glioma cell lines were derived from surgical resection material acquired from patients undergoing surgery at the Brigham and Women's Hospital on an Institutional Review Board-approved protocol as part of the DF/BWCC Living Tissue Bank. Briefly, tumor resection samples were mechanically dissociated and tumor spheres were established and propagated in Human NeuroCult NS-A Basal medium (StemCell Technologies) supplemented with epithelial growth factor, fibroblast growth factor, and heparin sulfate.

**Culture of human MSCs.** The use of human bone marrow aspirates followed a protocol approved by the Institutional Review Board of UMDNJ-Newark Campus. All subjects signed an informed consent. The ages of donors ranged between 18 and 35 years. MSCs were cultured from the aspirates as previously described.<sup>17</sup> Briefly, unfractionated bone marrow aspirates were diluted in Dulbecco's modified eagle medium (Invitrogen, Carlsbad, CA) containing 10% fetal calf

serum (Hyclone, Logan, UT) and then seeded in plasma-treated Falcon 3003 Petri dishes. The plates were incubated at 37 °C. On day 3, the mononuclear cells were selected by Ficoll Hypaque (Sigma, St Louis, MO) density gradient centrifugation and then replated on the culture plates. Fifty percent of the media were replaced with fresh media. At 80% confluence, the adherent cells were subjected to serial passages. At passage 5, the cells were CD45(-), CD14(-), CD44(+), CD29(+), CD105(+), and CD34(-).

**Mesodermal differentiation.** Adipogenic and osteogenic induction of MSCs was performed using Poietics Human Mesenchymal Stem Cells kit (Lonza, Switzerland). Briefly, MSCs were seeded in complete medium at a density of  $2 \times 10^4$ /cm<sup>2</sup> on plates treated with vacuum-gas plasma. Cells were allowed to adhere for 24 hours. The media were replaced at 72-hour intervals until confluence. The MSCs were induced as per manufacturers' instructions. Adipocyte staining was done using cells fixed in 10% formalin by incubation with 0.18% Oil Red O (Sigma) solution for 5 minutes. Osteogenic induction was based on mineralization of the bone. The induced cells were observed by bright-field microscopy at  $\times 100$ .

**Dye-transfer assay.** For this assay,  $5 \times 10^5$  cells were seeded in a 12-well plate. At adherence, 2.5  $\mu$ Mol/l of prewarmed CellTracker Orange CMTMR (Molecular Probes, Grand Island, NY) or CellTracker Green CMFDA (Molecular Probes) was added to the medium. The cells were incubated for 45 minutes at 37 °C in a CO<sub>2</sub> incubator. The cells were washed with phosphate-buffered saline (PBS) and then reincubated with fresh culture medium. After 6 hours, the cells were washed with PBS and cocultured with  $5 \times 10^5$  unlabeled cells. After 72 hours, the cells were trypsinized, harvested by centrifugation, resuspended in 0.5 ml of PBS, and then immediately evaluated by flow cytometry using a BD LSR II (BD Biosciences).

MSCs labeled with CMTMR were either cultured at 1:3 ratio with GBM cells for contact-dependent dye transfer or cultured in the upper chamber of a 0.4- $\mu$ m transwell culture system with CMFDA+ GBM cells in the lower chamber. Both culture methods spanned 72 hours.

**Real-time reverse transcriptase-PCR.** RNA was extracted using Trizol reagent (Invitrogen). Reverse transcription was performed with 200 ng of cDNA using Taqman MicroRNA Reverse Transcription Kit (Applied Biosystems, Foster City, CA) in accordance with the manufacturer's recommendation. Real-time PCR was performed on the 7300 Real-Time PCR System (Applied Biosystems) using the following parameters: an initial incubation of 50 °C for 2 minutes, followed by incubation at 95 °C for 10 minutes. The cycling conditions were as follows: 95 °C for 15 seconds and 60 °C for 60 seconds, for 40 cycles. Taqman miRNA expression kit was purchased from Applied Biosystems. miR expression was normalized with RNU6B expression. The relative expression was calculated using the 2(-Delta Delta C(T)) method, as previously described.<sup>19</sup>

**Western blot.** Whole-cell extracts were isolated using M-PER Mammalian Protein Extraction Reagent (Thermo Scientific, Danvers, MA). The extracts (3–7  $\mu$ g) were analyzed by

western blots on 12% sodium dodecylsulfate-polyacrylamide gel electrophoresis (SDS-PAGE) gels (Bio-Rad, Hercules, CA), as described.<sup>23</sup> Proteins were transferred onto polyvinylidene fluoride membranes (Perkin Elmer, Boston, MA). The membranes were incubated overnight with primary antibodies at final dilutions of 1/500–1/1,000. Primary antibodies were detected during a 2-hour incubation period with horse radish peroxidase conjugated immunoglobulin G at 1/2,000 final dilution. Horse radish peroxidase activity was detected by chemiluminescence using SuperSignal West Femto Maximum Sensitivity Substrate (Thermo Scientific). Membranes were stripped with Restore Stripping Buffer (Thermo Scientific) and then reprobbed for other proteins. Band density analyses were carried out using the Un-Scan-It software (Silk Scientific, Orem, UT).

**MDR1 knockdown.** To assess the importance of *MDR1* expression in GBM resistance to TMZ, U87 and T98G cells were transiently transfected with MDR1-RFP-C-RS (Origene Technologies, Rockville, MD). This vector constitutively expresses *MDR1* shRNA and Red Fluorescent Protein (RFP). Control GBM cells were transfected with nontargeting shRNA. Stable transfectants were selected by puromycin exposure (0.5  $\mu$ g/ml). The transfectants were treated with 200  $\mu$ Mol/l TMZ. At 72 hours, the cells were studied for caspase-3/7 activity using Vybrant FAM Caspase-3/7 Assay Kit (Invitrogen). Florescence was analyzed on the BD LSR II, after initially gating on RFP-expressing cells.

**Cell viability assay.** Cells were seeded at  $1.5 \times 10^4$ /well in triplicate and then treated with 200  $\mu$ Mol/l TMZ or vehicle. After 72 hours, cell viability was studied using the CellTiter-Blue Cell Viability Assay (Promega, Madison, WI).

**Isolation of exosomes.** Cell media were depleted of sera containing exosomes by overnight ultracentrifugation at 100,000 *g* and then stored at 4 °C. U87 and T98G cells (parental cells and cells overexpressing miR-9) were plated at  $5 \times 10^6$  per flask in standard media. After 24 hours, the cells were washed twice with PBS and then cultured with exosome-depleted media containing 200  $\mu$ Mol/l TMZ or vehicle. After 72 hours, the media were collected and then subjected to differential ultracentrifugation to isolate exosomes as described.<sup>27</sup> The media were first centrifuged at 2,000 *g* for 20 minutes to remove any live or dead cells. After this, the supernatant was transferred to a sterile tube for centrifugation at 10,000 *g* for 30 minutes to remove the remaining cell debris and large vesicles. The new supernatant was transferred to ultracentrifuge tubes and spun at 100,000 *g* for 80 minutes. The supernatant was disposed, and the exosome pellet was washed with PBS. A final spin was done at 100,000 *g* for 80 minutes, and the exosome pellet was resuspended in 100  $\mu$ l PBS. RNA was isolated from the exosomes with Trizol according to the manufacturer's instructions.

We also isolated exosomes using the Total Exosome Isolation kit from Invitrogen according to the manufacturer's protocol. The assays used exosome-cleared media, as described above, or sera-free media. The latter were used if the cells were stimulated for <24 hours. Prolonged experiments used exosome-cleared media with fetal calf serum.

**Statistical analyses.** Data were analyzed using the paired *t*-test for two comparable groups (control versus experimental). A *P* value <0.05 was considered significant.

### Supplementary material

#### Figure S1. Control studies on the effects of 1-octanol on GJIC.

1. Yamada, R and Nakano, I (2012). Glioma stem cells: their role in chemoresistance. *World Neurosurg* **77**: 237–240.
2. Chou, CW, Wang, CC, Wu, CP, Lin, YJ, Lee, YC, Cheng, YW et al. (2012). Tumor cycling hypoxia induces chemoresistance in glioblastoma multiforme by upregulating the expression and function of ABCB1. *Neuro-oncology* **14**: 1227–1238.
3. Bao, L, Hazari, S, Mehra, S, Kaushal, D, Moroz, K and Dash, S (2012). Increased expression of P-glycoprotein and doxorubicin chemoresistance of metastatic breast cancer is regulated by miR-298. *Am J Pathol* **180**: 2490–2503.
4. Abba, M, Mudduluru, G and Allgayer, H (2012). MicroRNAs in cancer: small molecules, big chances. *Anticancer Agents Med Chem* **12**: 733–743.
5. Martino, S, di Girolamo, I, Orlacchio, A, Datti, A and Orlacchio, A (2009). MicroRNA implications across neurodevelopment and neuropathology. *J Biomed Biotechnol* **2009**: 654346.
6. John-Aryankalayil, M, Palayoor, ST, Makinde, AY, Cerna, D, Simone, CB 2nd, Falduto, MT et al. (2012). Fractionated radiation alters oncomir and tumor suppressor miRNAs in human prostate cancer cells. *Radiat Res* **178**: 105–117.
7. Kim, TM, Huang, W, Park, R, Park, PJ and Johnson, MD (2011). A developmental taxonomy of glioblastoma defined and maintained by MicroRNAs. *Cancer Res* **71**: 3387–3399.
8. Schaich, M, Kestel, L, Pfirrmann, M, Robel, K, Illmer, T, Kramer, M et al. (2009). A MDR1 (ABCB1) gene single nucleotide polymorphism predicts outcome of temozolomide treatment in glioblastoma patients. *Ann Oncol* **20**: 175–181.
9. Auffinger, B, Thaci, B, Ahmed, A, Ulasov, I and Lesniak, MS (2013). MicroRNA targeting as a therapeutic strategy against glioma. *Curr Mol Med* **13**: 535–542.
10. Pendleton, C, Li, Q, Chesler, DA, Yuan, K, Guerrero-Cazares, H and Quinones-Hinojosa, A (2013). Mesenchymal stem cells derived from adipose tissue vs bone marrow: *in vitro* comparison of their tropism towards gliomas. *PLoS ONE* **8**: e58198.
11. Auffinger, B, Thaci, B, Nigam, P, Rincon, E, Cheng, Y and Lesniak, MS (2012). New therapeutic approaches for malignant glioma: in search of the Rosetta stone. *F1000 Med Rep* **4**: 18.
12. Bexell, D, Svensson, A and Bengzon, J (2013). Stem cell-based therapy for malignant glioma. *Cancer Treat Rev* **39**: 358–365.
13. Forbes, GM, Sturm, MJ, Leong, RW, Sparrow, MP, Segarajasingam, D, Cummins, AG et al. (2013). A phase 2 study of allogeneic mesenchymal stromal cells for luminal crohn's disease refractory to biologic therapy. *Clin Gastroenterol Hepatol*.
14. Greco, SJ and Rameshwar, P (2012). Mesenchymal stem cells in drug/gene delivery: implications for cell therapy. *Ther Deliv* **3**: 997–1004.
15. Matuskova, M, Hlubinova, K, Pastorakova, A, Hunakova, L, Altanerova, V, Altaner, C et al. (2010). HSV-tk expressing mesenchymal stem cells exert bystander effect on human glioblastoma cells. *Cancer Lett* **290**: 58–67.
16. Chagastelles, PC, Nardi, NB and Camassola, M (2010). Biology and applications of mesenchymal stem cells. *Sci Prog* **93**(Pt 2): 113–127.
17. Potian, JA, Aviv, H, Ponzio, NM, Harrison, JS and Rameshwar, P (2003). Veto-like activity of mesenchymal stem cells: functional discrimination between cellular responses to alloantigens and recall antigens. *J Immunol* **171**: 3426–3434.
18. Biancone, L, Bruno, S, Deregibus, MC, Tetta, C and Camussi, G (2012). Therapeutic potential of mesenchymal stem cell-derived microvesicles. *Nephrol Dial Transplant* **27**: 3037–3042.
19. Lim, PK, Bliss, SA, Patel, SA, Taborga, M, Dave, MA, Gregory, LA et al. (2011). Gap junction-mediated import of microRNA from bone marrow stromal cells can elicit cell cycle quiescence in breast cancer cells. *Cancer Res* **71**: 1550–1560.
20. Sun, AX, Crabtree, GR and Yoo, AS (2013). MicroRNAs: regulators of neuronal fate. *Curr Opin Cell Biol* **25**: 215–221.
21. Mao, H, Lebrun, DG, Yang, J, Zhu, VF and Li, M (2012). Deregulated signaling pathways in glioblastoma multiforme: molecular mechanisms and therapeutic targets. *Cancer Invest* **30**: 48–56.
22. Juszczak, GR and Swiergiel, AH (2009). Properties of gap junction blockers and their behavioural, cognitive and electrophysiological effects: animal and human studies. *Prog Neuropsychopharmacol Biol Psychiatry* **33**: 181–198.
23. Park, JM, Munoz, JL, Won, BW, Bliss, SA, Greco, SJ, Patel, SA et al. (2013). Exogenous CXCL12 activates protein kinase C to phosphorylate connexin 43 for gap junctional intercellular communication among confluent breast cancer cells. *Cancer Lett* **331**: 84–91.
24. Cogolludo, A, Moreno, L, Frazziano, G, Moral-Sanz, J, Menendez, C, Castañeda, J et al. (2009). Activation of neutral sphingomyelinase is involved in acute hypoxic pulmonary vasoconstriction. *Cardiovasc Res* **82**: 296–302.
25. Kucharzewska, P, Christianson, HC, Welch, JE, Svensson, KJ, Fredlund, E, Ringné, M et al. (2013). Exosomes reflect the hypoxic status of glioma cells and mediate hypoxia-dependent activation of vascular cells during tumor development. *Proc Natl Acad Sci USA* **110**: 7312–7317.
26. Oliva, CR, Moellering, DR, Gillespie, GY and Griguer, CE (2011). Acquisition of chemoresistance in gliomas is associated with increased mitochondrial coupling and decreased ROS production. *PLoS ONE* **6**: e24665.
27. Thery, C, Amigorena, S, Raposo, G and Clayton, A (2006). Isolation and characterization of exosomes from cell culture supernatants and biological fluids. *Curr Protocols Cell Biol* **30**: 3.22.1–3.22.29.



**Molecular Therapy–Nucleic Acids** is an open-access journal published by Nature Publishing Group. This work is licensed under a Creative Commons Attribution-NonCommercial-Share Alike 3.0 Unported License. To view a copy of this license, visit <http://creativecommons.org/licenses/by-nc-sa/3.0/>

Supplementary Information accompanies this paper on the Molecular Therapy–Nucleic Acids website (<http://www.nature.com/mtna>)